Composites Science and Technology 69 (2009) 335–342

Contents lists available at ScienceDirect

Composites Science and Technology

journal homepage: www.elsevier.com/locate/compscitech

Processing, characterization, and modeling of carbon nanotube-reinforced multiscale composites

Myungsoo Kim, Young-Bin Park *, Okenwa I. Okoli, Chuck Zhang

High-Performance Materials Institute, Florida A&M University – Florida State University, College of Engineering, 2525 Pottsdamer Street, Tallahassee, FL 32310, USA

ARTICLE INFO

Article history:
Received 25 June 2008
Received in revised form 28 August 2008
Accepted 15 October 2008
Available online 30 October 2008

Keywords:
A. Carbon nanotube
A. Hybrid composites
A. Nanocomposites
C. Modeling
D. Resin transfer molding (RTM)

ABSTRACT

Carbon fiber-reinforced epoxy composites modified with carbon nanotubes (CNTs) were fabricated and characterized. High-energy sonication was used to disperse CNTs in the resin, followed by infiltration of fiber preform with the resin/CNT mixture. The effects of sonication time on the mechanical properties of "multiscale" composites, which contain reinforcements at varying scales, were studied. A low CNT loading of 0.3 wt% in resin had little influence on tensile properties, while it improved the flexural modulus, strength, and percent strain to break by 11.6%, 18.0%, and 11.4%, respectively, as compared to the control carbon fiber/epoxy composite. While sonication is an effective method to disperse CNTs in a resin, duration, intensity, and temperature need to be controlled to prevent damages imposed on CNTs and premature resin curing. A combination of Halpin–Tsai equations and woven fiber micromechanics was used in hierarchy to predict the mechanical properties of multiscale composites, and the discrepancies between the predicted and experimental values are explained.

1. Introduction

The exceptional physical properties combined with high aspect ratios and low density render carbon nanotubes (CNTs) attractive for a new generation of multifunctional, high-performance engineering composites [1–5]. CNTs are considered an efficient filler material, as only a small loading in the resin, typically less than 5% by weight, can result in significant improvements in mechanical properties. A number of research groups performed studies on developing high-performance polymer composites containing CNTs, ranging between 0.1 and 5 wt% loading, and demonstrated significant improvements in tensile, shear, and flexural properties, fracture toughness, and thermal properties [5–11]. Studies have shown that the tensile modulus and yield strength of composites containing 1 and 4 wt% CNT can double and quadruple, respectively, as compared to neat resin samples [9]. CNTs also have been used to reinforce adhesives; one such study showed a nearly 50% enhancement in the average shear strength of an epoxy adhesive at 5 wt% loading of multiwalled nanotubes (MWCNTs) [10].

In recent years, fiber-reinforced polymer composites modified with CNTs, known as "multiscale" composite as they are reinforced with *microscale* fibers and *nanoscale* nanotubes [12,13], have drawn significant attention in the field of advanced, high-performance materials. Most of the efforts in multiscale composites research have been focused on improving the matrix-dominated properties by dispersing CNTs in the bulk of the matrix. High-energy sonication has been widely used to "predisperse" CNTs in the resin prior to composite fabrication [14–19]. However, more recently, calendering has gained popularity as a means to disperse CNTs due to its efficiency and scalability, which makes it suitable for high volume, high rate production [7,8,20–23]. Calendering utilizes adjacent cylindrical rollers rotating at different velocities to generate high shear stresses, and is commercially used for dispersing pigments in inks, paints, and cosmetics [8]. As for integrating resin/CNT mixture and fiber fabric, resin transfer molding (RTM)/vacuum-assisted resin transfer molding (VARTM) [20,23,24] and hand layup [14,15] are commonly used. Although improvements in mechanical properties of multiscale composites have been achieved with the addition of CNTs, the transferability of improved matrix properties into continuous-fiber-reinforced composites is a challenging task and limited by many factors [23].

An allied area of recent research development is modeling of carbon nanotube composites and multiscale composites to predict the mechanical properties. Currently, for carbon nanotube composites, Halpin–Tsai equations [25–29] and Mori–Tanaka method [29–32] are widely used. Qian [27] considered the MWCNT/polystyrene composite films as randomly oriented discontinuous fiber lamina and calculated the tensile modulus of the composite using Halpin–Tsai equations. In another study [28], modified Halpin–Tsai equations were proposed to evaluate the tensile modulus and strength of MWCNT/phenolic composites by adopting orientation and exponential shape factors.

Several micromechanics models have been proposed to obtain the mechanical properties of woven fiber-reinforced composites

* Corresponding author. Tel.: +1 404 513 6655; fax: +1 850 410 6342.
E-mail address: ypark.me03@gtalumni.org (Y.-B. Park).

0266-3538/$ - see front matter © 2008 Elsevier Ltd. All rights reserved.
doi:10.1016/j.compscitech.2008.10.019

[33–37]. Woven fibers consist of repeating unit cells. Elastic properties of repeating unit cells can be considered as the composite properties because repeating unit cells represent the architecture of woven fiber composite [36]. For the strength of repeating unit cells, including tensile and compressive strengths, several failure criteria can be used, such as the von Mises and Tsai-Wu failure criteria [34]. The ultimate tensile strength can be predicted based on the transverse tensile load and in-plane shear load [36].

This paper presents a study that combines processing, characterization, and modeling of carbon fiber-reinforced epoxy composites and carbon nanotube-reinforced multiscale composites. VARTM was employed as the composite manufacturing method, and high energy sonication was used as the primary means to achieve CNT dispersion in the matrix. Sonication conditions were varied to investigate the effects of sonication parameters on the resin infusion behavior and the resulting mechanical properties of the composites. The matrix–fiber–nanotube interfaces, which govern the load transferability, were explored through scanning electron microscopy (SEM). In parallel, Halpin–Tsai equations and woven fiber micromechanics were combined to develop a unified model that predicts the upper bound of the tensile properties. The experimental work lays the groundwork for a systematic study that optimizes the sonication process for maximized composite performance.

2. Experimental

2.1. Materials

The carbon nanotubes (CNTs) used in this study were XD-grade characterized by the electrical conductivity suitable for electrostatic discharge application, manufactured by Unidym Inc. XD-grade CNTs are a mixture of single-, double-, and triple-walled nanotubes [38]. Raman spectroscopy was performed on the as-received XD nanotubes using inVia Reflex developed by Renishaw. The Raman spectra obtained using a 785-nm-wavelength laser is shown in Fig. 1a. The spectra show the characteristic tangential mode band (i.e., G band near 1590 cm^{-1}) of single-walled nanotubes (SWCNTs), indicating SWCNT dominance. However, a small intensity disruption in the increasing slope of the G band peak, typical in SWCNTs, is absent. The intensity of the disorder band (i.e., D band near 1300 cm^{-1}) is relatively high compared to SWCNTs, indicating partially defective graphitic structure. The spectra are quite different from typical MWCNTs or vapor grown carbon nanofibers, which show noisy curves and D band intensities higher than G band intensities [39]. In summary, as the XD CNTs are a mixture of SWCNTs and MWCNTs, the Raman spectra show the characteristics of both, resembling that of double-walled nanotubes.

An atomic force microscope (AFM; MultiMode II by Veeco Digital Instruments Group) was used to quantify the diameters of the nanotubes. First, a nanotube suspension was produced by dispersing the nanotubes in distilled water with the aid of a surfactant. Dispersion was achieved by sonication (Sonicator 3000 from Misonix Corporation). Several drops of suspension were applied on to a silicon substrate and were allowed to dry in open air, leaving nanotube agglomerates. Fig 1b shows the images of nanotube-surfactant aggregates as seen under the AFM. The rope diameter ranges from 10 to 30 nm in the localized areas represented by the images.

The four-harness satin weave IM7 carbon fiber obtained from Hexcel was used as the preform. The matrix material consisted of Epon 862 epoxy resin and EpiCure W curing agent manufactured by Miller-Stephenson Chemical Co.

2.2. Fabrication process

First, precalculated amounts of CNTs and curing agent were weighed and mixed together in a beaker, such that the weight fraction of CNTs was 0.3% with respect to resin and curing agent. Tip sonication was employed to disperse the CNTs in the curing agent for 30 min. During the sonication process, the beaker containing the mixture was submerged in an ice bath to prevent it from heating up. After sonication, the EpiCure W/CNT mixture was combined with Epon 862 and the three-component mixture was sonicated further. To investigate the effect of sonication duration for the three-component mixture, two sonication conditions were applied – 10 min and 3 h. The stoic mixture ratio of Epon 862 and EpiCure W was 100:26.4, as suggested by the manufacturer. Upon completion of the sonication process, the mixture was degassed in a vacuum oven at room temperature for 30 min and was subsequently preheated to 50 °C before infusing into fiber mold. The schematic illustration of the vacuum-assisted resin transfer molding (VARTM) setup is shown in Fig. 2. Four layers of carbon fiber fabric,

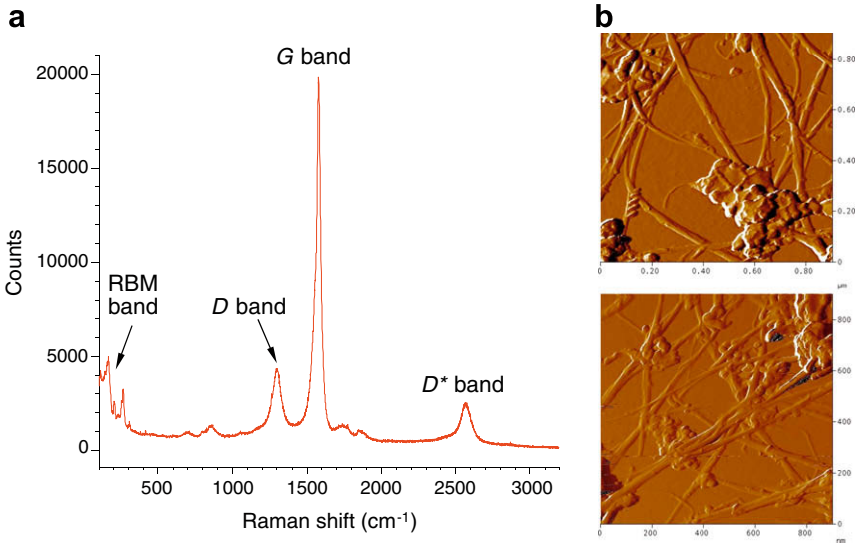

Fig. 1. Characterization of as-received XD-grade CNTs: (a) Raman spectra under 785 nm laser wavelength and (b) AFM images (each image captures a 1 μm by 1 μm area).

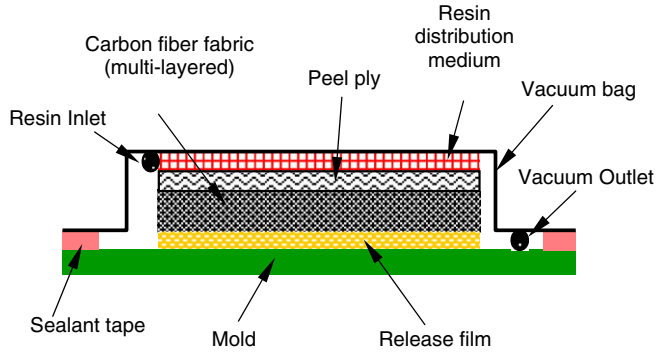

Fig. 2. Schematic of VARTM setup.

each measuring approximately 305 mm by 305 mm, were stacked in alternating warp-fill directions. Once the fiber preform was infiltrated with Epon 862/EpiCure W/CNT mixture, it was allowed to cure at 121 °C for 2 h and post-cure at 177 °C for 2 h. In this study, three fiber-reinforced panels were fabricated – one control panel with neat resin (Panel 1) and two panels with 0.3 wt% CNT dispersed resin sonicated for 10 min and 3 h, respectively (Panels 2 and 3).

2.3. Sample characterization

Tensile and flexural specimens were prepared and tests were performed in accordance with ASTM D3039 and D790, respectively. An MTS test machine (Model 858 table top system) equipped with a 25 kN load cell was used. From each composite panel, dog-bone-shaped tensile specimens (254 mm in overall length, 12.7 mm wide in narrow section, and 1 mm in thickness) and rectangular flexural specimens (50.8 mm in length, 12.7 mm in width, and 1 mm in thickness) were cut using garnet-abrasive-assisted water-jet cutting (OMAX 55100). Tensile tests were performed at a crosshead speed of 2 mm/min until specimens failed, and a laser extensometer was used to measure the strains *in situ*. Flexural tests were performed under the displacement controlled, three-point bending mode at a span length of 25.4 mm and a crosshead speed of 1 mm/min until specimens failed. The morphology of the fracture surfaces of the composite samples were observed using the JEOL JSL-7401F scanning electron microscope (SEM) to investigate the fiber–matrix interfaces and CNT dispersion in the matrix.

3. Micromechanics modeling

To predict the material properties of multiscale composites, Halpin–Tsai equations and woven fiber micromechanics were used in hierarchy (Fig. 3). First, for mechanical properties of carbon nanotube composites, Halpin–Tsai equations were applied. The carbon nanotube composite properties were then utilized to compute the mechanical properties of multiscale composites using woven fiber micromechanics. In woven fiber micromechanics, the mechanical properties of carbon nanotube composites were used as the properties of the matrix.

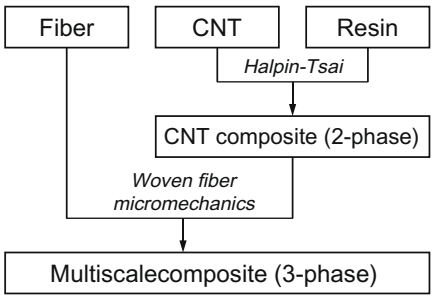

Fig. 3. Schematic of composite hierarchy for computation of mechanical properties of multiscale composites.

3.1. Halpin–Tsai equations

One of the prerequisites for obtaining the mechanical properties of a resin/fiber/CNT multiscale composite is to compute the material properties of the resin/CNT composite. In this work, Halpin–Tsai equations were used to predict the bulk properties of the carbon nanotube composite. The Halpin–Tsai equations are a set of empirical relationships that enable the property of a composite material to be expressed in terms of the properties of the matrix and reinforcing phases together with their proportions and geometry. The Halpin–Tsai equation that yields the tensile modulus of a nanocomposite can be expressed as [7,26,40]

$$E_{NC} = \left[\frac{3}{8}\frac{1+2(l_{NT}/d_{NT})\eta_L V_{NT}}{1-\eta_L V_{NT}} + \frac{5}{8}\frac{1+2\eta_D V_{NT}}{1-\eta_D V_{NT}}\right]E_{epoxy}$$
$$\eta_L = \left(\frac{(E_{NT}/E_{epoxy})-(d_{NT}/4t)}{(E_{NT}/E_{epoxy})+(l_{NT}/2t)}\right) \quad (1)$$
$$\eta_D = \left(\frac{(E_{NT}/E_{epoxy})-(d_{NT}/4t)}{(E_{NT}/E_{epoxy})+(d_{NT}/2t)}\right)$$

where E, l_{NT}, d_{NT}, V_{NT} and t represent the tensile modulus, the length and outer diameter of the nanotubes, nanotube volume fraction, and thickness of graphite layer (0.34 nm), respectively. Since the XD-grade nanotubes are a mixture of single- and multiwalled nanotubes, the parameters were calculated based on the assumed mixed ratio on weight, 1:2 of SWCNTs and MWCNTs. The volume fractions of SWCNTs and MWCNTs were calculated to be 0.089% and 0.178% based on the CNT and epoxy densities of 1.35 g/cc and 1.2 g/cc [4,41,42], respectively. The estimated diameter, length, and modulus of SWCNTs are 1.4 nm, 25 μm, and 640 GPa, respectively. The estimated MWCNT diameter, length, and Young's modulus of 20 nm, 50 μm and 400 GPa were used in the calculation, respectively [2].

Eq. (1) yields the epoxy/CNT composite tensile modulus of 2.95 GPa at 0.3 wt% CNT loading, which translates to a 8.46% increase from the neat epoxy modulus of 2.72 GPa [41,42]. In this calculation, the carbon nanotube composites were regarded as isotropic, as the CNTs were assumed to be uniformly distributed and randomly oriented through the matrix. As the amount of CNTs was small, the Poisson's ratio of the carbon nanotube composite was assumed to be the same as that of epoxy, 0.33 [41,42]. Based on the isotropy assumption, the shear modulus can be calculated using Eq. (2) which expresses the relation between tensile and shear moduli [41,42].

$$G_{NC} = \frac{E_{NC}}{2(1+\nu)} \quad (2)$$

where G_{NC} is shear modulus of carbon nanotube composite and ν is Poisson's ratio. Table 1 shows the results of material properties of neat epoxy and carbon nanotube composite. At 0.3 wt% CNT loading, shear modulus increased by 8.82%.

Table 1
Material properties of neat epoxy and epoxy/0.3 wt% CNT composite.

CNT concentration	Tensile modulus, E (GPa)	Poisson's ratio (ν)	Shear modulus, G (GPa)
Neat resin (0 wt%)	2.72	0.33	1.02
CNT composite (0.3 wt%)	2.95	0.33	1.11

3.2. Woven fiber micromechanics

Several micromechanics models have been proposed to predict the mechanical properties of woven fiber composites [33–36]. Woven fibers consist of repeating unit cells. The material properties of repeating unit cells can be used as the composite properties because repeating unit cells represent the architecture of woven fiber composite. The goal of micromechanics of woven fiber composites in this study was to obtain the stiffness matrices of the multiscale composite, as shown in Eq. (3), which are the relationships between the in-plane stress and moment resultants and the in-plane strains and curvature [33].

$$\begin{Bmatrix} N_i \\ M_i \end{Bmatrix} = \begin{bmatrix} A_{ij}(x,y) & B_{ij}(x,y) \\ B_{ij}(x,y) & D_{ij}(x,y) \end{bmatrix} \begin{Bmatrix} \varepsilon_j^0 \\ \kappa_j \end{Bmatrix} \quad (i,j = 1,2,6) \tag{3}$$

$$A_{ij}(x,y), B_{ij}(x,y), D_{ij}(x,y) = \int_{-h/2}^{h/2} (1, z, z^2) Q_{ij}^I \, dz \tag{4}$$

where the superscript I refers to either fill strand (F), warp strand (W), or matrix (M). Q_{ij}^I is evaluated for each constituent of the composite unit cell. Therefore, the warp and fill strands, matrix, and the fiber undulation in the warp and fill strands are taken into consideration.

From the $[A]$, $[B]$ and $[D]$ matrices in Eq. (3), the effective tensile moduli, shear modulus, and Poisson's ratios of the woven composite can be obtained as [33]

$$E_x = A_{11}^* - \frac{A_{12}^{*\,2}}{A_{22}^*}, \quad E_y = A_{22}^* - \frac{A_{12}^{*\,2}}{A_{11}^*}, \quad \nu_{xy} = -\frac{A_{12}^*}{A_{22}^*}, \quad G_{xy} = A_{66}^* \tag{5}$$

where $[A^*] = [A]/h$, and h is the composite thickness.

As mentioned earlier, four-harness satin weaves were used in this study. To simulate the strand configuration, the following form of undulation along the x axis was assumed for the median fiber of the fill strand

$$H_f(x) = \left\{ -\frac{h_f}{2} \sin\left(\frac{\pi x}{a}\right) \cup -\frac{h_f}{2} \right\} \quad 0 \le x \le 4a \tag{6}$$

For the undulation of the median fiber of the warp strand, Eq. (7) was used

$$H_w(y) = \left\{ \frac{h_w}{2} \sin\left(\frac{\pi y}{a}\right) \cup \frac{h_w}{2} \right\} \quad 0 \le y \le 4a \tag{7}$$

In Eqs. (6) and (7), subscripts f and w denote fill and warp strands, respectively, and h and a are strand thickness and width, respectively. The equations were implemented in a simulation code using MATLAB to generate the geometrical configurations of a four-harness satin weave fabric, as shown in Fig. 4.

The volume fraction of a woven fiber-reinforced composite can be expressed as [33]

$$v_f = v_{f/s} \frac{4 h_s L_s}{a h \pi} \tag{8}$$

where $v_{f/s}$ is the fiber volume fraction in the strands, h_s is the strand thickness, and L_s is the undulation length. In the experimental work that was performed in this study, the fiber volume fraction of Panel 1, that is, the control epoxy/carbon fiber composite panel (see Section 2.2), was measured to be $v_f = 0.51$ from a simple weighing method. Table 2 shows the geometric parameters of the repeating unit cell of the epoxy/carbon fiber composite.

Table 2
Geometrical parameters of the repeating unit cell of epoxy/IM7 four-harness satin weave carbon fiber composite.

Geometrical parameter	Value
Width of the fill and warp strand (mm)	$a_w = a_f = 1.60$
Maximum thickness of the fill and warp strand (mm)	$h_w = h_f = 0.14$
Thickness of the unit cell (mm)	$h = 0.28$
Fiber volume fraction in the strand	$V_{f/s} = 0.8$

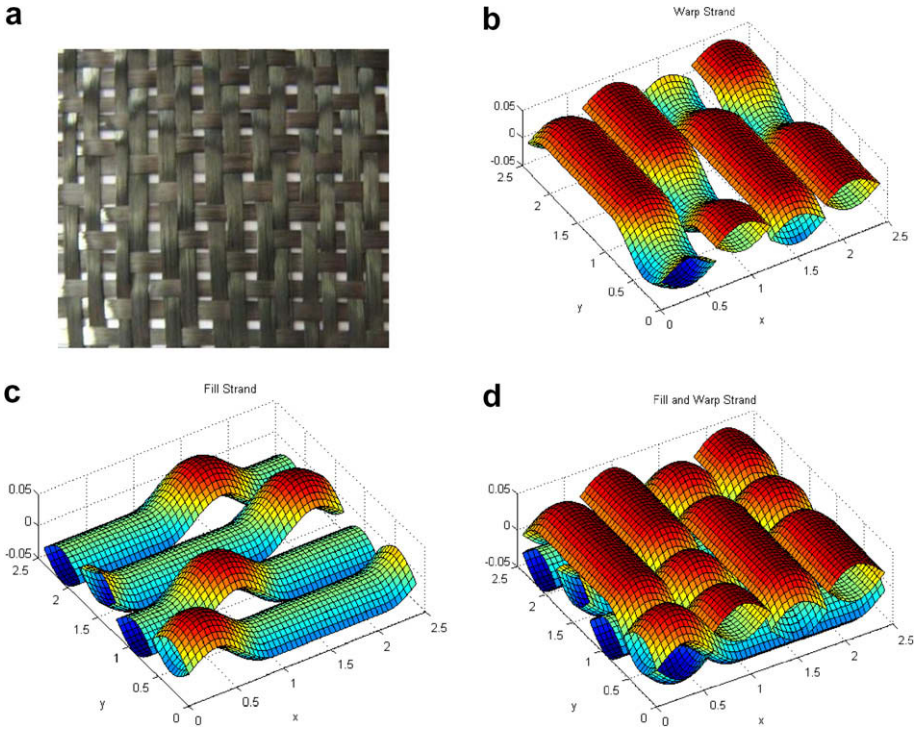

Fig. 4. Geometrical configurations of IM7 carbon fiber fabric: (a) closed-up photograph of IM7 four-harness satin weave carbon fiber; (b) warp strands in the computer-generated model; (c) fill strands in the computer generated model, and (d) fill and warp strand in the computer generated model.

Table 3
Mechanical properties of epoxy/carbon fiber composite and epoxy/carbon fiber/CNT multiscale composite strands with a carbon fiber volume fraction of 0.8.

Mechanical property	Epoxy/carbon fiber composite	Epoxy/carbon fiber/CNT composite
Longitudinal tensile modulus, E_{11} (GPa)	221.3	221.4
Transverse tensile modulus, E_{22} (GPa)	13.08	14.15
In-plane shear modulus, G_{12} (GPa)	4.94	5.34
In-plane Poisson's ratio	0.226	0.226

The width and thickness parameters of the strands were measured using an optical microscope (Olympus BX40 and analySIS imager). Eq. (8) yields the fiber volume fraction in the strand, v_{fs}, of 0.8. Each strand was considered as a unidirectional fiber-reinforced composite and the mechanical properties of strands were calculated by CADEC, a micromechanics software provided by [42]. Table 3 shows the mechanical properties of the epoxy/carbon fiber composite and epoxy/carbon fiber/CNT multiscale composite strands. For multiscale composite strands, the mechanical properties of the carbon nanotube composites were used as matrix properties. The mechanical reinforcement of the epoxy matrix using CNTs resulted in moderate improvements in transverse tensile modulus and in-plane shear modulus, while longitudinal tensile modulus was not affected. The increase in transverse tensile modulus with the inclusion of CNTs is attributed to the CNT reinforcing effect in the transverse direction, which is matrix-dominated. Nonetheless, it has negligible influence in the longitudinal direction, which is fiber-dominated. The in-plane shear modulus was also enhanced by CNTs, as they reinforce the inter-filament epoxy matrix in the composite strand against shear in the longitudinal direction.

4. Experimental results and discussions

4.1. Composite panel fabrication

Sample panels 1, 2, and 3 were fabricated using VARTM, as described in Section 2.2. A photograph capturing the infusion of the Epon 862/EpiCure W/0.3 wt% CNT mixture through four layers of carbon fiber preforms for Sample 2 is shown in Fig. 5. For all the samples, a flow distribution medium was used to facilitate the resin flow and to maintain an even flow front. The resin mixtures used to infiltrate fiber fabrics for Samples 2 and 3 exhibited markedly different viscosities upon sonication (10 min and 3 h of sonication, respectively), resulting in significantly longer infusion time for Sample 3. The times it took for the resin mixture to flow from the inlet to the vacuum outlet and infiltrate the fiber preforms were approximately 40 min and 2 h, respectively. (The infusion time for Sample 1 was approximately 20 min.) The increase in the viscosity after prolonged (3 h) sonication may be due to premature gelling partially assisted by heating that has been generated due to the intense sonication condition. The effects of infusion viscosity on the mechanical properties are discussed in the following section.

4.2. Effect of nanoreinforcement on mechanical properties

The in-plane tensile moduli and strengths obtained from mechanical tests are shown in Fig. 6a and b, and Table 4. In Fig. 6a, "Models 1 and 2" denote theoretical tensile moduli for epoxy/carbon fiber (using woven fiber micromechanics) and epoxy/carbon fiber/CNT composites (using a combination of Halpin–Tsai equations and woven fiber micromechanics), respectively. "Panel 1" denotes experimentally obtained tensile properties for epoxy/carbon fiber composites, and "Panels 2 and 3" denote those for epoxy/carbon fiber/CNT composites processed after 10 min and 3 h sonication, respectively. Each test involved six test coupons, except the tensile test for Panel 1, for which four coupons were tested. The results presented in Fig. 6 are mean values with standard deviation bars. Models 1 and 2 are not shown in Fig. 6b, as the theoretical models employed in this study do not apply to tensile strength.

In the case of epoxy/carbon fiber composite, the theoretical tensile modulus is larger than the measured value by 11.8%. The discrepancy is due to the assumptions implicated in the Halpin–Tsai equations and woven fiber micromechanics, namely, perfect fiber-matrix bonding and zero inter-strand (or inter-tow) gap. The carbon fiber–epoxy interface was investigated by observing the morphology at the fracture surface using SEM. The SEM images shown in Fig. 7 illustrate weak bonding at the fiber–matrix interface. The arrows in Fig. 7b and d indicate the evidence of fiber–matrix debonding and fiber pull-out.

The inter-strand gap also contributes to the reduction in the measured tensile modulus of the composite. The carbon fiber fabric used in this study is marked by loosely woven fiber structure as can be observed in Fig. 4a. It is reported that a 4% gap size with respect to the strand width can result in a 22% main stiffness reduction as compared to a no-gap fiber fabric [36]. Panels 1–3 show similar tensile moduli and strengths, as these properties are dominated by the fiber reinforcement rather than the matrix. Moreover, the low CNT loading of 0.3 wt% has a minimal influence on the composite properties as confirmed by the theoretical tensile moduli, which showed a mere 1.39% increase (from Model 1 to Model 2) with the addition of CNTs. On the other hand, in Table 4, the improvement in the theoretical in-plane shear modulus is

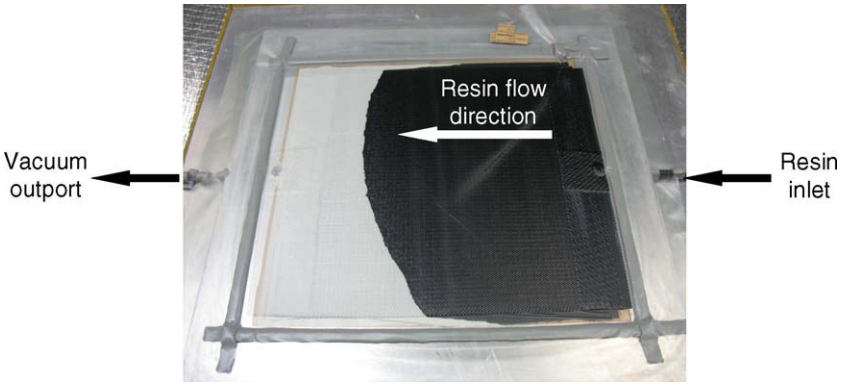

Fig. 5. Photograph taken during vacuum-assisted infusion of resin/curing agent/CNT mixture (Panel 2).

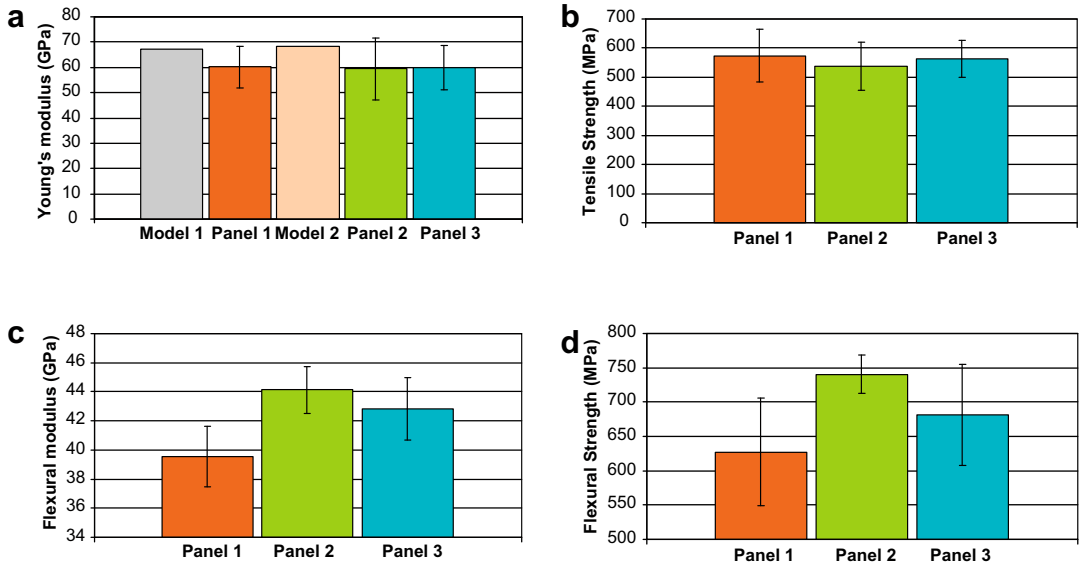

Fig. 6. Effect of sonication time on mechanical properties of epoxy/carbon fiber/CNT multiscale composites ("Models 1 and 2" denote theoretical tensile moduli for epoxy/carbon fiber and epoxy/carbon fiber/CNT composites, respectively. "Panel 1" denotes experimentally obtained properties for epoxy/carbon fiber composites, and "Panels 2 and 3" denote those for epoxy/carbon fiber/CNT composites processed after 10 min and 3 h sonication, respectively): (a) tensile modulus; (b) tensile strength; (c) flexural modulus, and (d) flexural strength.

Table 4
Comparison of predicted and experimental values of mechanical properties of neat and CNT-modified carbon fiber-reinforced epoxy composites.

		In-plane Tensile modulus (GPa)	In-plane Tensile Strength (MPa)	Flexural modulus (GPa)	Flexural strength (MPa)	In-plane Shear modulus (GPa)	Poisson's ratio
Epoxy/CF composite	Model 1	67.3	–	–	–	3.5483	0.0203
	Panel 1	60.2 ± 8.2	574.1 ± 76.5	39.5 ± 2.1	627.4 ± 78.2	–	–
Epoxy/CF/CNT multiscale composite	Model 2	68.3	–	–	–	3.8394	0.0217
	Panel 2	59.4 ± 12.3	532.1 ± 91.6	44.1 ± 1.6	740.6 ± 27.4	–	–
	Panel 3	59.9 ± 8.9	562.7 ± 62.8	42.8 ± 2.1	681.5 ± 73.2	–	–

much greater (8.20%), which is attributed to the fact that in-plane shear is significantly affected by the matrix reinforcement.

On the contrary, Fig. 6c and d show moderate improvements in the flexural modulus and strength with the inclusion of CNTs. When compared with Panel 1, Panels 2 and 3 show 11.6% and 8.4% increase in flexural modulus, and 18.0% and 8.6% increase in flexural strength, respectively. The enhancements are due to the reinforcing effects of the nanotubes, as flexural properties are matrix-dominated rather than fiber-dominated. A notable trend is that Panel 2 exhibits greater improvements than Panel 3, indicating the sonication time for CNT dispersion in epoxy/curing agent mixture may have an effect on the final flexural properties of the multiscale composites. Fig. 8 shows the representative SEM images obtained from the fracture surfaces of Panels 2 and 3. 10 min sonication resulted in poor dispersion, characterized by CNT aggregates (Fig. 8a), while 3 h sonication yielded generally well dispersed and distributed CNTs (Fig. 8b). The reduced mechanical properties in Panel 3, when compared with Panel 2, infer that there exists a more dominant factor than the degree of CNT dispersion that governs the matrix-dominated mechanical properties. Another competing mechanism may be the degree of cure of the epoxy resin at the time of infusion. As mentioned previously, the epoxy/carbon fiber/CNT mixture after 3 h sonication has high viscosity. The high viscosity of the mixture tends to prohibit complete fiber wetting, as it is more difficult for the partially crosslinked polymer molecules to conform to the fiber preform and infiltrate the inter-strand and inter-filament spaces. In addition to sonication time, heat build-up generated during prolonged sonication may have contributed to premature curing, and this possibility warrants further investigation.

To take maximum advantage of the reinforcing effect of CNTs, it is crucial to achieve strong nanotube–matrix interfacial bonding. In particular, it is important to reinforce the interface between the fiber and the matrix using CNTs so that the load can be transferred between the two and at the same time the gap between the highly mismatched properties of matrix and fiber can be bridged [21]. The pulled out nanotubes in Fig. 8 indicate weak interfacial bonding between epoxy and nanotubes. Although sonication is one of the most widely employed methods to disperse CNTs in a resin, it still lacks processing guidelines, which should be established through a systematic experimental study accompanied by the understanding of underlying physics. For infusion purposes, it is necessary to optimize the sonication process such that balance can be maintained between the degree of CNT dispersion, damages imposed on the CNTs (particularly shortening of nanotubes under severe sonication conditions), and mixture viscosity due to premature curing. The experimental study addressing this issue is currently being performed by the authors.

5. Conclusions

In this study, epoxy/carbon fiber/CNT multiscale composite panels were produced using sonication and VARTM. A small loading of CNTs (0.3 wt% with respect to the resin/curing agent mix-

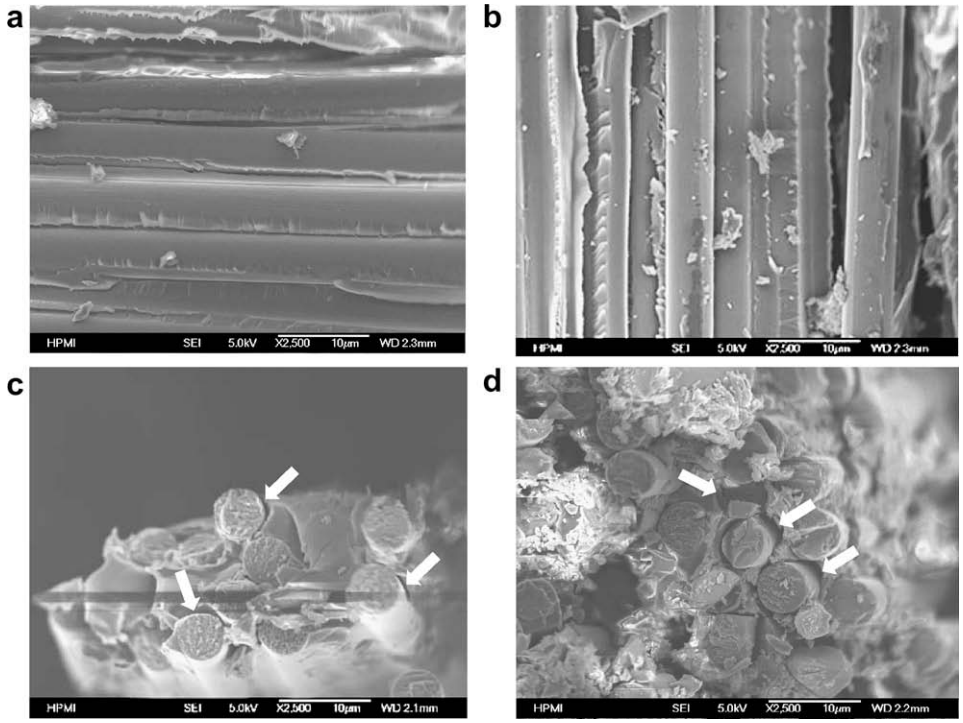

Fig. 7. SEM images of carbon fiber–epoxy interfaces in Panel 1 (a, b) and Panel 2 (c, d): (a) longitudinal debonding (Panel 1); (b) fiber pull-out and debonding (Panel 1); (c) longitudinal debonding (Panel 2), and (d) fiber pull-out and debonding (Panel 2).

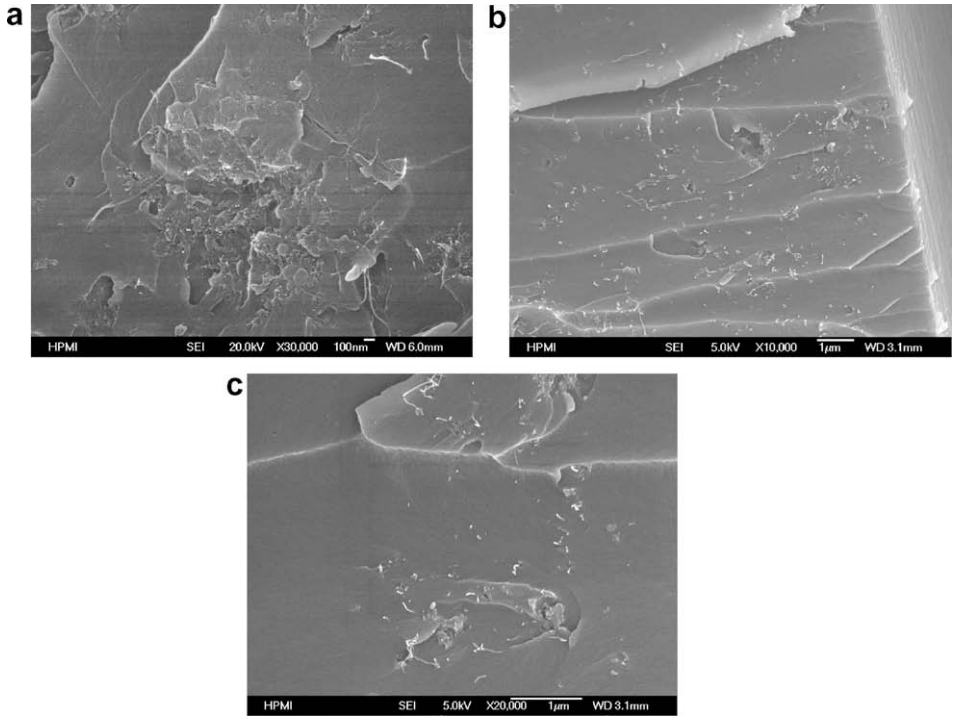

Fig. 8. SEM images of fracture surfaces of epoxy/carbon/fiber/CNT composites showing: (a) CNT aggregates in Panel 2; (b) well dispersed CNTs in Panel 3; and (c) the pulled out CNTs in Panel 3.

ture) had little influence on the fiber-dominated tensile properties, while it enhanced the matrix-dominated flexural properties significantly. It was demonstrated that CNTs can serve as an efficient filler material that can reinforce the matrix at a small loading. However, SEM analysis revealed weak bonding at the matrix–fiber–nanotube interfaces, suggesting that load transferability has

a room for improvement. Optimizing the sonication process will help maximize CNT dispersion while minimizing damages imposed on the CNT and preventing premature curing. However, pretreating the fiber or chemically functionalizing the CNTs may be necessary to enhance the interfacial strength.

Multiscale composite modeling was performed in parallel to predict the tensile properties. The Halpin–Tsai equations and woven fiber micromechanics were combined to capture the geometrical configuration of the woven structure and to integrate the nanomodified matrix properties into the multiscale composite properties. The developed model showed a tendency to overestimate the properties and therefore may be utilized by the composite designers as a tool to obtain the upper bound. Efforts are currently being made by the authors to modify the models by relaxing the assumptions so that the properties can be predicted more accurately.

Acknowledgments

The authors would like to acknowledge the financial and technical support from the High-Performance Materials Institute at Florida State University. Thanks are also due to Mr. Jerry Horne and Dr. Xinyu Fan, who assisted in performing VARTM and mechanical testing, respectively.

References

[1] Esawi AMK, Farag MM. Carbon nanotube reinforced composites: potential and current challenges. Mater Des 2007;28(9):2394–401.
[2] Baughman H, Zakhidov AA, de Heer WA. Carbon nanotubes – the route toward applications. Science 2002;197:787–92.
[3] Liu L, Wagner HD. Rubbery and glassy epoxy resins reinforced with carbon nanotubes. Compos Sci Technol 2005;65:1861–8.
[4] Thostenson ET, Li C, Chou TW. Nanocomposites in context. Compos Sci Technol 2005;65:491–516.
[5] Lau KT, Shi SQ. Failure mechanisms of carbon nanotube/epoxy composites pretreated in different temperature environments. Carbon 2002;40:2965–8.
[6] de Villoria RG, Miravete A, Cuartero J, Chiminelli A, Tolosana N. Mechanical properties of SWNT/epoxy composites using two different curing cycles. Compos Part B 2006;37:273–7.
[7] Gojny FH, Wichmann MHC, Köpke U, Fiedler B, Schulte K. Carbon nanotube-reinforced epoxy-composites: enhanced stiffness and fracture toughness at low nanotube content. Compos Sci Technol 2004;64:2363–71.
[8] Thostenson ET, Chou TW. Processing-structure-multi-functional property relationship in carbon nanotube/epoxy composites. Carbon 2006;44:3022–9.
[9] Allaoui A, Bai S, Cheng HM, Bai JB. Mechanical and electrical properties of a MWNT/epoxy composite. Compos Sci Technol 2002;62:1993–8.
[10] Hsiao KT, Alms J, Advani SG. Use of epoxy/multiwalled carbon nanotubes as adhesives to join graphite fibre reinforced polymer composites. Nanotechnology 2003;14:791–3.
[11] Zhou Y, Pervin F, Lewis L, Jeelani S. Experimental study on the thermal and mechanical properties of multi-walled carbon nanotube-reinforced epoxy. Mater Sci Eng A 2007;452–453:657–64.
[12] Thostenson EST, Li WZ, Wang DZ, Ren ZF, Chou TW. Carbon nanotube/carbon fiber hybrid multiscale composites. J Appl Phys 2002;91(9):6034–7.
[13] Bekyarova E, Thostenson ET, Yu A, Kim H, Gao J, Tang J, et al. Multiscale carbon nanotube-carbon fiber reinforcement for advanced epoxy composites. Langmuir 2007;23:3970–4.
[14] Iwahori Y, Ishiwata S, Sumizawa T, Ishikawa T. Mechanical properties improvements in two-phase and three-phase composites using carbon nano-fiber dispersed resin. Compos Part A 2005;36:1430–9.
[15] Liao YH, Liang Z, Park YB, Wang B, Zhang C. Fabrication and characterization of carbon nanotube/glass fiber-reinforced multiscale composites. In: 47th AIAA/ASME/ASCE/AHS/ASC Structures, Structural Dynamics, and Materials Conference, Newport, RI, 2006.
[16] Zhou Y, Pervin F, Lewis L, Jeelani S. Fabrication and characterization of carbon/epoxy composites mixed with multi-walled carbon nanotubes. Mater Sci Eng A 2007;452–453:657–64.
[17] Puglia D, Valentini L, Kenny JM. Analysis of the cure reaction of carbon nanotubes/epoxy resin composites through thermal analysis and Raman spectroscopy. J Appl Polym Sci 2003;88:452–8.
[18] Kim B, Lee J, Yu I. Electrical properties of single-wall carbon nanotube and epoxy composites. J Appl Phys 2003;94(10):6724–8.
[19] Liao YH, Marietta-Tondin O, Liang Z, Zhang C, Wang B. Investigation of the dispersion process of SWNTs/SC-15 epoxy resin nanocomposites. Mater Sci Eng A 2004;385:175–81.
[20] Gojny FH, Wichmann MHG, Fiedler B, Bauhofer W, Schulte K. Influence of nano-modification on the mechanical and electrical properties of conventional fibre-reinforced composites. Compos Part A 2005;36:1525–35.
[21] Gojny FH, Wichmann MHG, Fiedler B, Schulte K. Influence of different carbon nanotubes on the mechanical properties of epoxy matrix composites – a comparative study. Compos Sci Technol 2005;65(15–16):2300–13.
[22] Gojny FH, Wichmann MHG, Fiedler B, Kinloch I, Bauhofer W, Windle AH. Evaluation and identification of electrical and thermal conduction mechanisms in carbon nanotube/epoxy composites. Polymer 2006;47:2036–45.
[23] Wichmann MHG, Sumfleth J, Gojny FH, Quaresimin M, Fiedler B, Schulte K. Glass-fibre-reinforced composites with enhanced mechanical and electrical properties – benefits and limitations of a nanoparticle modified matrix. Eng Fract Mech 2006;73:2346–59.
[24] Thostenson ET, Chou TW. Carbon nanotube network: sensing of distributed strain and damage for life prediction and self healing. Adv Mater 2006;18:2837–41.
[25] Halpin JC, Kardos JL. The Halpin–Tsai equations: a review. Polym Eng Sci 1976;16(5):344–52.
[26] Peeterbroeck S, Breugelmans L, Alexandre M, BNagy J, Viville P, Lazzaroni R, et al. The influence of the matrix polarity on the morphology and properties of ethylene vinyl acetate copolymers-carbon nanotube nanocomposites. Compos Sci Technol 2007;67:1659–65.
[27] Qian D, Dickey EC, Andrews R, Rantell T. Load transfer and deformation mechanisms in carbon nanotube–polystyrene composites. Appl Phys Lett 2000;76(20):2868–70.
[28] Yeh MK, Tai NH, Liu JH. Mechanical behavior of phenolic-based composites reinforced with multi-walled carbon nanotubes. Carbon 2006;44:1–9.
[29] Li X, Gao H, Scrivens WA, Fei D, Xu X, Sutton MA, et al. Reinforcing mechanisms of single-walled carbon nanotube-reinforced polymer composites. J Nanosci Nanotechnol 2007;7:2309–17.
[30] Seidel GD, Lagoudas KC. Micromechanical analysis of the effective elastic properties of carbon nanotube reinforced composites. Mech Mater 2006;38:884–907.
[31] Jiang B, Liu C, Zhang C, Wang B, Wang Z. The effect of non-symmetric distribution of fiber orientation and aspect ratio on elastic properties of composites. Compos Part B 2007;38:24–34.
[32] Mori T, Tanaka K. Average stress in matrix and average elastic energy of materials with misfitting inclusions. Acta Metall 1973;21:571–4.
[33] Scida D, Aboura Z, Benzeggagh ML, Bocherens E. Prediction of the elastic behavior of hybrid and non-hybrid woven composites. Compos Sci Technol 1997;57:1727–40.
[34] Scida D, Aboura Z, Benzeggagh ML, Bocherens E. A micromechanics model for 3D elasticity and failure of woven-fibre composite materials. Compos Sci Technol 1999;59:505–17.
[35] Aitharaju VR, Averill RC. Three-dimensional properties of woven-fabric composites. Compos Sci Technol 1999;59:1901–11.
[36] Huang ZM. The mechanical properties of composites reinforced with woven and braided fabrics. Compos Sci Technol 2000;60:479–98.
[37] Zako M, Uetsuji Y, Kurashiki T. Finite element analysis of damaged woven fabric composite materials. Compos Sci Technol 2003;63:506–16.
[38] Tao K, Yang S, Grunlan JC, Kim YS, Dang B, Deng Y, et al. Effects of carbon nanotube fillers on the curing processes of epoxy resin-based composites. J Appl Polym Sci 2006;102(6):5248–54.
[39] Chae HG, Sreekumar TV, Uchida T, Kumar S. A comparison of reinforcement efficiency of various types of carbon nanotubes in polyacrylonitrile fiber. Polymer 2005;46:10925–35.
[40] Thostenson ET, Chou TW. On the elastic properties of carbon nanotube-based composites: modeling and characterization. J Phys D: Appl Phys 2003;36:573–83.
[41] Mallick PK. Fiber-reinforced composites materials manufacturing and design. 2nd ed. vols. 18–19. New York NY: Marcel Dekker Inc.; 1993 p. 50–56.
[42] Barbero EJ. Introduction to composite materials design. vol. 17. New York NY: Taylor & Francis; 1999 p. 29.